Geophysical Research Letters

RESEARCH LETTER
10.1029/2020GL092071

Key Points:

- Acidic droplets with pH <3 formed in wet plumes are emitted from coal-fired stationary sources
- The SO_4^{2-} concentrations in plumes grow explosively and are 2.8~3.3 times higher than those in stacks
- SO_2 aqueous-phase oxidation process is critical in sulfate aerosol formation via plume droplets

Supporting Information:

- Supporting Information S1

Correspondence to:
Q. Li,
qli@fudan.edu.cn

Citation:
Ding, X., Li, Q., Wu, D., Wang, X., Li, M., Wang, T., et al. (2021). Direct observation of sulfate explosive growth in wet plumes emitted from typical coal-fired stationary sources. *Geophysical Research Letters*, *48*, e2020GL092071. https://doi.org/10.1029/2020GL092071

Received 22 DEC 2020
Accepted 23 FEB 2021

Direct Observation of Sulfate Explosive Growth in Wet Plumes Emitted From Typical Coal-Fired Stationary Sources

Xiang Ding[1], Qing Li[1,2], Di Wu[1], Xiaoyan Wang[3], Mei Li[4,5], Tao Wang[6], Lin Wang[1], and Jianmin Chen[1,2,3]

[1]Shanghai Key Laboratory of Atmospheric Particle Pollution and Prevention, Department of Environmental Science and Engineering, Fudan University, Shanghai, China, [2]Shanghai Institute of Eco-Chongming (SIEC), Shanghai, China, [3]Department of Atmospheric and Oceanic Sciences & Institute of Atmospheric Sciences, Fudan University, Shanghai, China, [4]Institute of Mass Spectrometry and Atmospheric Environment, Guangdong Provincial Engineering Research Center for Online Source Apportionment System of Air Pollution Jinan University, Guangzhou, China, [5]Guangdong-Hong Kong-Macau Joint Laboratory of Collaborative Innovation for Environmental Quality, Guangzhou, China, [6]Department of Civil and Environmental Engineering, Hong Kong Polytechnic University, Hong Kong, China

Abstract The origins of atmospheric sulfate production have previously been explained by focusing on air quality models and complex chemical reaction processes. Here, we first report direct observations of sulfate production in stack plumes discharged from coal-fired power plants, industrial boilers, and sintering plants equipped with wet desulfurization systems. Less than one third of the particulate SO_4^{2-} in plumes is attributed to dust-SO_4^{2-} and SO_3 measured in stacks. The SO_2 aqueous-phase oxidation process is critical in explaining the unknown sulfate formation in plume droplets with pH values ranging from 2.3 to 2.8. When the rapidly formed sulfate in wet plumes is included, a notable amount of underestimated sulfate (~0.24 Tg in 2017) is emitted from industrial stacks in China and can partially explain the "missing sulfate" on driving most particle pollution episodes. Policy-making targeting particulate emissions is suggested to substantially reduce sulfate emissions for further air quality improvement.

Plain Language Summary Sulfate aerosols are well known as an important atmospheric aerosol component, especially during haze periods. Their production pathway remains a mystery, and they are also referred to as missing sulfate. We show that sulfuric acid droplets are readily produced in wet plumes emitted from typical coal-fired stationary sources. The freshly formed sulfate originates from the condensation and absorption of SO_2 and SO_3 emitted from stacks when the discharged flue gas cools in ambient air. We discover that the fast-formed sulfate aerosols in the wet plumes from industrial stacks account for ~31.4% of the directly emitted sulfate aerosols in China. This study advances our understanding of industrial particulate emissions and their contribution to atmospheric sulfate.

1. Introduction

Sulfate (SO_4^{2-}) has been recognized as a key and major component of fine particulate matter (PM) with an aerodynamic diameter of 2.5 μm or smaller ($PM_{2.5}$) in the atmosphere, especially during severe haze events (Cheng et al., 2016; Huang et al., 2014; Shah et al., 2018). SO_4^{2-} directly impacts the solar radiative balance and the physicochemical properties of aerosols (Tsigaridis & Kanakidou, 2018). Ground-based observations from 2005 to 2014 have revealed that the averaged proportions of sulfate in the atmospheric $PM_{2.5}$ mass are 15% ± 6% and 20% ± 5% in northern and southern China, respectively (Zhang et al., 2017). The SO_4^{2-} concentration has been intensively studied via modeling by mainly focusing on its formation through atmospheric SO_2 oxidation (secondary formation) to determine a sufficient chemical production mechanism (R. Zhang et al., 2015). However, a knowledge gap (also referred to as missing sulfate) remains in regards to our understanding of the sources and formation pathways of high SO_4^{2-} concentrations, especially during Chinese winter haze periods (Huang et al., 2014; Shah et al., 2018; Y. X. Wang et al., 2014; Zhang et al., 2017; Zheng et al., 2020).

Atmospheric sulfate sources, except secondary formation, have also recently been reported to be directly attributed to primary emissions from combustion sources, such as coal combustion in households and

industry (Dai et al., 2019; Ding et al., 2019; Z. Li et al., 2017; B. Wu et al., 2018). A source apportionment study has revealed that ~37% of the particulate sulfate during winter haze periods is directly emitted from coal combustion in Xi'an and Beijing (Huang et al., 2014). Coal combustion is also the major anthropogenic source of sulfate precursor (SO_2 and SO_3) emissions (Geng et al., 2017; Tang et al., 2019). However, the particulate sulfate, and SO_2 emission amounts have been dramatically reduced by the implementation of ultralow emission (ULE) standards over the past decade in China, especially regarding coal-fired power plants (CFPPs) (Karplus et al., 2018; Tang et al., 2019; Tong et al., 2018). China's annual CFPP emitted SO_2 and PM dropped by 65% and 72%, respectively, between 2014 and 2017 (Tang et al., 2019).

Although the concentration of SO_2 is strictly controlled by the integrated system of wet flue gas desulfurization (WFGD) and wet electrostatic precipitation (WESP), SO_2 is still the predominant soluble gas in the wet plumes (also known as white plumes) (Seigneur et al., 2011; Wu et al., 2020), which surrounded by saturated water vapor will immediately condense into solid and liquid particles in the elevated stack plumes (Feng et al., 2018). The favorable conditions for SO_2 to dissolve in droplets and generate $S_{(IV)}$ include (1) a large number of microdroplets, (2) a high SO_2 uptake coefficient at a low temperature, (3) a long uptake response time provided by the large stack space, and (4) a relatively uniform distribution of droplets and SO_2. The highest $S_{(IV)}$ concentration and instantaneous microdroplet amount in a fresh plume may be generated when the flue gas column leaves the stack outlet along with a dramatic decrease in the flue gas temperature. Aircraft field measurements have identified that sulfate may be formed during the aging process of CFPP plumes via aqueous-phase SO_2 oxidation (Dittenhoefer & De Pena, 1980; Green et al., 2019; Kim et al., 2017; Luria et al., 2001). However, direct evidence for the sulfate emission and formation in real-world plumes is still lacking.

This study represents a first important step toward the quantitative estimation of the sulfate emissions from coal-fired stationary sources based on systematic chemical analysis and real-world investigation of plumes emitted from stack outlets. Freshly formed droplets along wet plume edges were collected using a modified fog collector in the wintertime. Furthermore, the characteristics of flue gases before/after FGDs were also comparatively investigated, as well as the freshly formed PM originating from white plumes. The sulfate formation process in plumes was also examined to provide a key to uncovering the missing sulfate formation pathway during winter haze periods.

2. Materials and Methods

2.1. Sampling Units

Field measurements were conducted at three types of representative stationary sources (including four power plants, one industrial boiler, and two steel sinters, Figure S1). CFPPs and industrial boilers account for the majority of coal consumption in China, and they are two of the major emission sources of atmospheric SO_2 and PM. The installed capacities of the four tested ULE CFPPs range from 24 to 680 MW. The air pollution control devices (APCDs) installed in these CFPPs occur in sequence with selective catalytic reduction (SCR) units, ESP units, WFGD units, and WESP units for further PM removal. A widely used limestone-based WFGD system is installed in CFPPs #1, #2, and #3, while a seawater-based WFGD is employed in offshore CFPP #4. A ULE retrofit was implemented in the tested industrial circulating fluidized bed (CFB) boiler with a capacity of 75 t/h, and it contains the same APCDs, including a limestone-based WFGD unit. The two tested sintering machines, iron ore smelting processes of with coal as fuel typical in the steel industry, exhibit an area of 360 m^2 with installed ESP, limestone (sinter #1)/ammonia-based WFGD (sinter #2), and WESP units. The tested utility/industrial boilers, sintering areas, installed APCDs and fuel properties are detailed in Table S1 and our previous studies (Ding et al., 2019, 2020; Liang et al., 2020).

2.2. Sampling Methods and Field Measurements

Droplet along plume edges were collected with a modified single-stage Caltech active strand cloud-water collectors version 2 (CASCC2), which has been widely applied in the collection of atmospheric cloud-water samples (J. Li et al., 2017; Rattigan et al., 2001). The modified CASCC2 instrument (Figure S2) drew droplets at a flow rate of 5.8 m^3 min^{-1}. Droplets with diameters larger than 3.5 μm were efficiently impacted on Teflon filaments, while any escaped droplets and PM were filtered with a coupled Teflon filter (Whatman),

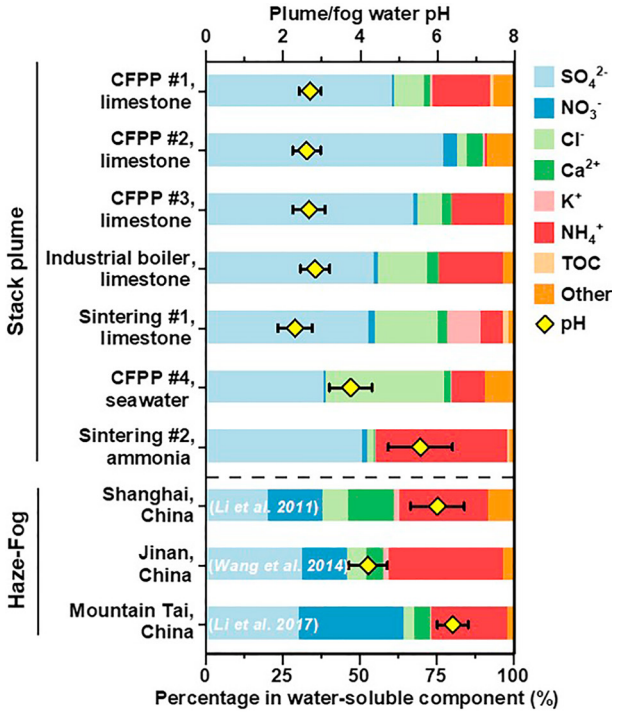

Figure 1. Water-soluble compositions and pH of the sampled droplets in the plumes discharged from the stack exits into ambient air. The stack plume samples are collected from typical stationary combustion sources, including coal-fired power plants, industrial boilers, and steel sintering plants equipped with wet desulfurization systems. The data on three haze-fog events in China (Li et al., 2011, J. Li et al., 2017; X. Wang et al., 2014) are shown for comparsion.

which occurred between the Teflon filaments and fan in the CASCC2. Plume droplets were captured via the combination of filaments and filter, and collected into a 500 mL high-density polyethylene bottle. The pH value and $S_{(IV)}$ content of the collected droplet samples were immediately (within 10 min) analyzed in the field via a portable pH meter (model 6350M, JENCO) and an ultraviolet-visible (UV) spectrophotometer at 570 nm, respectively. The droplet size distribution (0.5–2,000 μm) and velocity distribution at the plume edges were monitored online with a Doppler phase interferometer (PDI-TK1).

PM, $PM_{2.5}$, and SO_3/H_2SO_4 were collected at both the WFGD inlets and outlets in each tested plant with an ESC-5000 isokinetic sampling system (Environmental Supply Company) according to USEPA methods 201 and 8A. A single particle aerosol mass spectrometer (SPAMS, Hexin Instrument Co., Ltd.) was employed in the field to analyze the chemical composition of individual aerosols immediately (5~10 min) after direct collection at the WFGD inlet, WFGD outlet, and stack outlet at CFPP #1 by utilizing a 10L vacuum quartz-glass bottle designed specifically for particle sampling. The markers and ions used to identify 4 types of particles (accounting for 98.8% of the total sulfate particle number) are detailed in Table S2. The SPAMS performance and data analysis process are detailed in previous literature (Yang et al., 2017; Zhou et al., 2020). A brief introduction of this instrument, chemical analysis of collected samples, and quality control in this study are provided in the supporting information Text S1.

3. Results and Discussion

3.1. Acid Droplets Emitted From Stacks as White Plumes

Figure 1 shows the measured acidity and water-soluble composition of the collected droplets along typical stack plume edges discharged from the tested CFPPs, industrial boilers, and steel sintering plants. The pH of the stack plume water ranged from 2.3 to 5.6. The seawater WFGD shows less acidic, possibly owing to the excess seawater spray in the tower and a much lower temperature after desulfurization, leading to relatively low condensable PM (CPM) emissions. Ammonia functions as a neutralizer in the ammonia WFGD system, which is thus less acidity. When the saturated flue gases (46°C~58°C) originating from the limestone WFGD systems are discharged into the ambient air (−12°C~8°C), the formed droplets are extremely acidic with pH values ranging from 2.3 to 2.8, which are more acidic than those emitted from the plants equipped with the other two WFGD systems. The dominant ions are SO_4^{2-}, Cl^-, and NH_4^+ with volume-weighted mean concentrations of 1,245 ± 1,058, 181 ± 129, and 683 ± 837 mg/L aq, respectively, which cumulatively accounted for 81%~96% of the total determined ion concentrations. Except for the dust emitted from stacks directly contributing to the dominant ions, a large amount of soluble gaseous species (including SO_X, HCl, and NH_3) quickly condenses and/or dissolves into the plume droplets, and thus contributes to the water-soluble components. In the extremely acidic plumes emitted from the limestone WFGD systems, SO_4^{2-} even accounts for more than half (53%~77%) of the water-soluble components. Both SO_4^{2-} and acidity levels of the plume droplets are 2~3 orders of magnitude higher than those of the cloud water observed during the haze-fog events in China (X. Wang et al., 2014; Xue et al., 2016).

The absolute water content (AWC) increased by 22%~209% in the limestone WFGD systems with the mass concentrations in the WFGD outlets ranging from 94~167 g/Nm^3, equivalent to 12%–16% of the flue gas volume (Table S3). Owing to the much lower temperature of ambient air, especially during the winter period, the saturated wet flue gases formed in WFGD towers could generate droplets upon discharge into ambient air, resulting in so-called white plume. The mean values of the droplet number widely ranged from 2.9×10^5 to 4.1×10^7 #/cm^{-3}, while their sizes ranged from 0.2 to 17.8 μm with the median value of 2.1 μm (Figure S3).

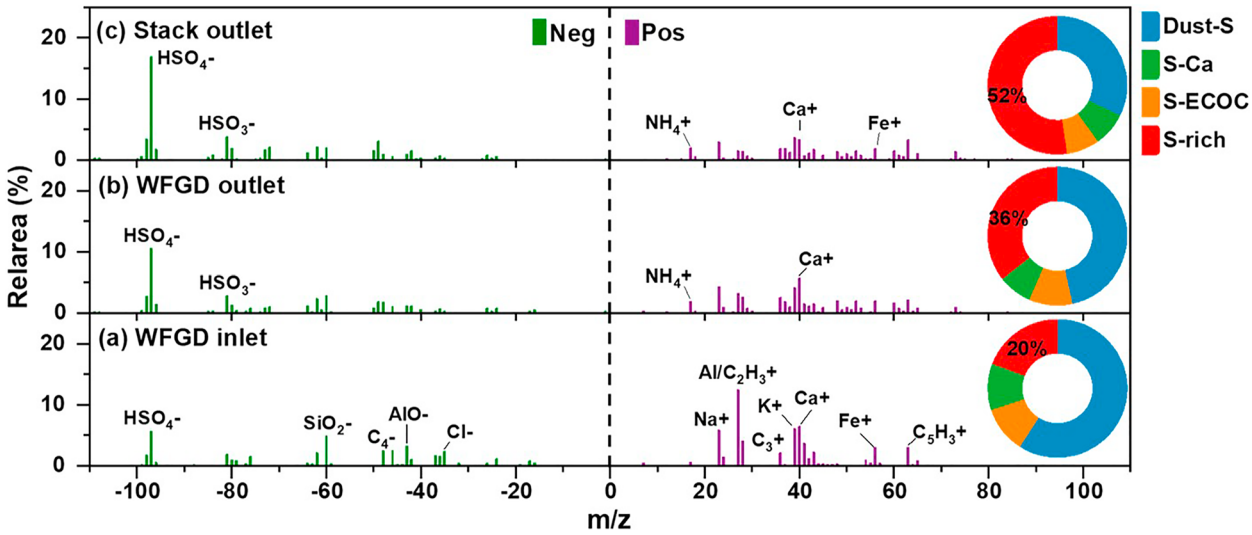

Figure 2. Average mass spectra of the single particles at the (a) WFGD inlet, (b) WFGD outlet, and (c) stack outlet in CFPP #1. The single particles emitted from the CFPP contain four major type particles, including dust-sulfate (Dust-S), sulfate-calcium (S-Ca), sulfate-elemental and organic carbon (S-ECOC), and sulfate-rich (S-rich) particles. The number shown in the inserted pie part indicates the relative contribution of the S-rich particles to the total particle count.

3.2. Formation of SO_4^{2-} From Wet FGD and Aqueous Absorption

PM precursors can be converted into the particulate phase and thus affect the aerosol chemical composition during the cooling processes of flue gases, including at WFGD inlet, WFGD outlet, and stack outlet, as indicated by the SPAMS results depicted in Figure 2. In regard to the single sulfate-containing particles at the WFGD inlet (129°C), Dust-S particles contributed 54.8% of the total sulfate-containing particles, followed by S-rich (20.0%), S-Ca (10.3%), and S- elemental and organic carbon (ECOC) (9.1%) particles, as shown in the pie charts. When the flue gas temperature decreased to 48°C at the WFGD outlet and further decreased to the ambient temperature (5°C) at the stack outlet, the abundance of the S-rich particles continuously increased, and they became the major component, accounting for 52.1% of the total sulfate-containing particles at the stack outlet, while the relative contributions of the Dust-S, S-Ca, and S-ECOC particles continuously decreased.

The average mass spectra of the single particles at the WFGD inlet, WFGD outlet, and stack outlet of the selected CFPPs further demonstrated that the relative content of sulfate ($^{96}SO_4^-$) increased with increasing flue gas cooling (Figure 2). High $^{23}Na^+$, $^{36}C_3^+$, $^{40}Ca^+$, $^{56}Fe^+$, and $^{63}C_5H_3^+$ intensities are shown in the positive ion model at the WFGD inlet, while strong $^{35}Cl^-$, $^{43}AlO^-$, $^{60}SiO_2^-$, $^{48}C_4^-$ (EC), and $^{96}SO_4^-$ signals are detected in the negative ion model (Figure 2a). These peaks indicate that the aerosols at the WFGD inlet are directly formed during combustion in the CFPP boiler (fly ash), consistent with our previous study on CFPP emissions (Ding et al., 2019). The fractions of the sulfate and sulfite clusters including $^{97}HSO_4^-$, $^{96}SO_4^-$, $^{81}HSO_3^-$, and $^{80}SO_3^-$, were much higher in the negative ion spectrum at the WFGD outlet, while the signals of $^{17}NH_4^+$ and $^{40}Ca^+$ slightly increased owing to the conversion of NH_3 and WFGD slurries. The S-rich particles exhibited a submicron size distribution at the WFGD outlet with a unimodal size distribution, while the peak located at 0.6 μm (Figure S4). The relative concentration of SO_4^{2-} in PM increased from 7.8% at the WFGD inlet to 13.6% at the WFGD outlet (Table S3). The characteristics of the ionic compositions during the cooling processes agree well with the off-line sample analysis. The increase in sulfite species ($^{81}HSO_3^-$ and $^{80}SO_3^-$) through further cooling processing at the stack outlet potentially provides an additional explanation for the measured relative high content of S-rich particles. A discussion of the stack-outlet particle analysis is provided in the supporting information Text S2.

3.3. In-Plume SO_2 Oxidation Pathway

The conversion process of SO_4^{2-} from SO_2 and SO_3 in the stack outlet (plume edge) was examined at three selected coal-fired stationary sources, as shown in Figure 3a. The contribution of fly ash containing SO_4^{2-}

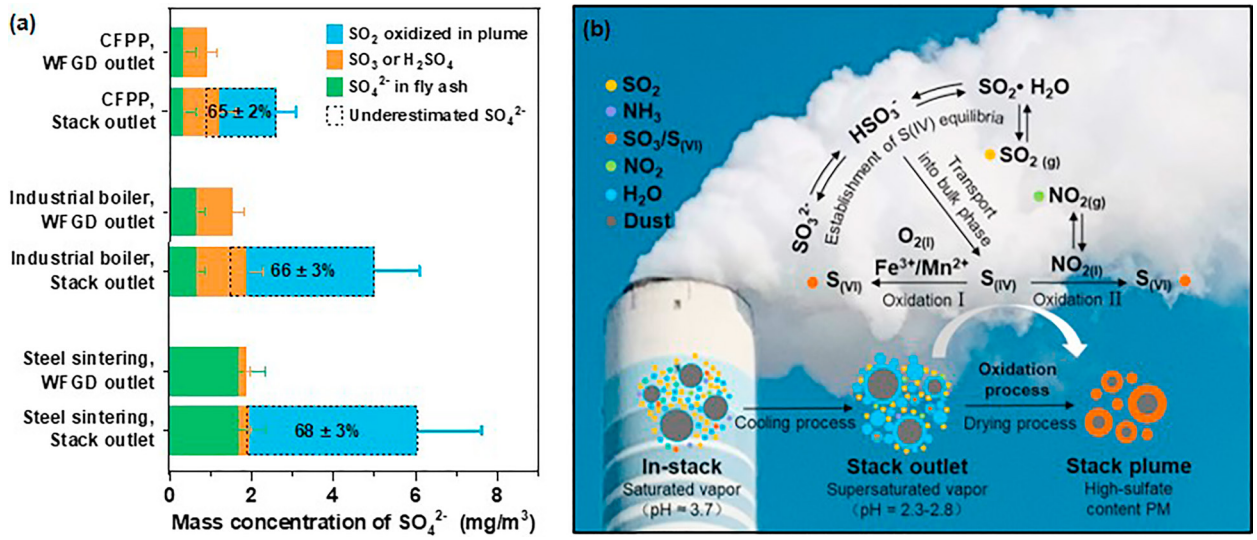

Figure 3. (a) Mass concentrations of the total SO_4^{2-} at the WFGD and stack outlets of the three typical coal-fired stationary sources; (b) schematic diagram of fast sulfate production through oxidation of $S_{(IV)}$ by dissolved NO_2 and TMI-catalyzed oxidation in the stack plume. The mass concentrations of the total SO_4^{2-} at the stack outlets include all sulfate particles and SO_3 after the desulfurization systems.

(including dust-S, S-Ca, and S-ECOC particles), H_2SO_4/SO_3 condensation, and SO_2 oxidation are distinguished by the determination of the fly ash, H_2SO_4/SO_3, and SO_2 concentrations, respectively, at the WFGD outlets according to EPA method 8A. Fly ash containing SO_4^{2-} originating from stacks may directly contribute to the in-plume sulfate, while H_2SO_4/SO_3 could readily generate sulfuric acid aerosols upon flue gas cooling. The relative contributions of H_2SO_4/SO_3 to the total in-stack sulfate at the WFGD outlet are 63%, 56%, and 12% in the CFPPs, industrial boilers, and steel sintering plants, respectively. Due to the low SO_3 concentration emitted during the sintering process, its relative contribution is low. Compared to the in-stack sulfate concentrations, the in-plume SO_4^{2-} concentrations increased by 1.8, 2.2 and 2.3 times in the CFPPs, industrial boilers, and steel sintering plants, respectively. A notable significant increase was also reported in many studies and explained as the condensation of emitted CPM and SO_3. The concentration of condensable sulfate in the CFPP stacks obtained by the dry impinger method (EPA method 202/201A) varied widely within the range of 0.56~4.23 mg/m^3 (Feng et al., 2018; G. Wang et al., 2020; Wu et al., 2020). Most of these reported values obtained by the dry impinge method are commonly lower than the concentration of the increased sulfate as measured in the CFPP plumes. Additionally, the WFGD-outlet SO_3 and fly ash SO_4^{2-} cumulatively account for less than one third of the in-plume SO_4^{2-} for each wet stack in this study. Many model studies suggested that in-cloud oxidation greatly contributes (60%–90%) to the total sulfate budget (Dovrou et al., 2019; Ervens, 2015; Harris et al., 2013). Thus the contribution of another sulfate precursor, that is, SO_2, is the key to explaining the fast formation of these unknown sulfates in stack plumes.

Attainment of a comprehensive understanding of the oxidation path of $S_{(IV)}$ in plumes is a major challenge, similar to that in atmospheric cloud-fog, which is attributed to multiple pathways of atmospheric SO_2 oxidation in aqueous-phase systems, include reactions with dissolved O_3, H_2O_2, NO_2, and transition-metal ion (TMI)-catalyzed O_2 (Gen et al., 2019; J. Wang et al., 2020). Due to the absence of photolysis in plumes, only TMIs ($Fe_{(II/III)}$ and $Mn_{(II/III)}$) in the PM and NO_2 produced by combustion occur in the emitted plumes. The rate of TMI-catalyzed $S_{(IV)}$ oxidation is independent of the oxygen concentration (Connick & Zhang, 1996); therefore, the aqueous-phase $S_{(IV)}$ oxidation processes in the stack plumes can be classified as two pathways, that is, oxidation by NO_2 and TMI-catalyzed O_2 oxidation (Figure 3b). Referring to the rate calculation equations summarized in Table S4, the $S_{(IV)}$ oxidation rates in the stack plumes under the two pathways in the CFPPs, industrial boilers, and steel sintering plants are listed in Table S5. The calculated total production rate at pH <3 ranged from 0.02 to 0.39 mg/m^3/s with a mean value of 0.11 mg/m^3/s in the stack plumes, which is 10^4~10^5 times higher than that estimated during the Chinese haze events with ~10 μg/m^3/h level (Dallosto & Harrison, 2006; Lei et al., 2020). The production rate of the steel sintering sector is much higher than that of the other two sectors, because the flue gases from sintering plants contain a high TMI contents

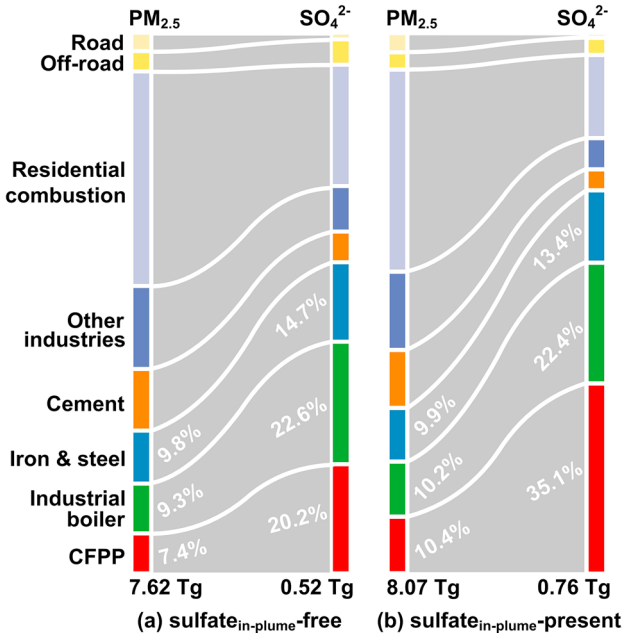

Figure 4. (a) Emission percentages of $PM_{2.5}$ and sulfate across source sectors, and (b) Reassessed emission percentages of $PM_{2.5}$ and sulfate (including the underestimated part for industrial wet stacks) in 2017 for the nationwide of mainland China. China's anthropogenic $PM_{2.5}$ emissions (including 8 sectors, i.e., CFPP, industrial boiler, iron & steel, cement, other industries, residential combustion, off-road, and road transport) in 2017 are adopted from the framework of the Multiresolution Emission Inventory for mainland China (MEIC, http://www.meicmodel.org) (Zheng et al., 2018). Annual anthropogenic sulfate emission was obtained by multiplying the primary $PM_{2.5}$ emission values in the 8 sectors with the corresponding mass fractions as listed in Figure S5. There are uncertainties on estimating anthropogenic sulfate emissions mainly due to the difference of temporal and spatial distribution coefficients, and the difference in mass fraction values of each sectors in different regions (Chen et al., 2021; Reff et al., 2009). The emissions from CFPP, industrial boiler and iron & steel in the MEIC were respectively divided into with-WFGD and without-WFGD systems, while their apportion coefficients of $PM_{2.5}$ to their corresponding categories were adopted from our previous study (Ding et al., 2020).

(Fe^{3+} and Mn^{2+}), whose pathway contributes the most (~99.5%) to the total SO_4^{2-} production rate (0.39 mg/m^3/s). The TMI pathway contributes more than 96% to the overall sulfate production rate in all studied plumes, while the NO_2 oxidation pathway contributes only a small fraction to the overall sulfate production rate. The overall calculated sulfate production rate under the above oxidation pathways agrees well with the measurements, but the calculated results underestimate the sulfate production rate in the studied CFPPs by ~ 44%. A detailed simulation and analysis is required in the future, including the heterogeneous reaction of SO_2 with slipped NH_3 from the denitration processes for reducing NOx concentrations. The two oxidation pathways involved highlight the possibility of rapid SO_4^{2-} formation in plumes, which may enhance the atmospheric SO_4^{2-} loading.

3.4. Contribution of Sulfate Condensation to the Ambient Air

Figure S5 shows the average mass percentage of SO_4^{2-} in $PM_{2.5}$ in the stacks and fresh plumes, based on the assumption that all the discharged microdroplets directly produce $PM_{2.5}$ after the drying process for all plants. Previous studies on fine particulate sulfate emissions from various anthropogenic sources are included for comparison. The SO_4^{2-} percentages in $PM_{2.5}$ determined at the WFGD outlet are consistent with the previously reported values. However, the particulate SO_4^{2-} percentages in $PM_{2.5}$ formed via wet plume processes are notably higher than all the reported results based in-stack measurements. The highest SO_4^{2-} percentages contained in $PM_{2.5}$ were detected in the CFPPs, mainly due to the efficient removal of nonsulfate particles (fly ash, OC, and EC) by the deployment of ULE APCDs in China. Because the sulfur content in coal is much higher than that in biomass and most fuel oil (Lu et al., 2011), the coal sector (including industrial and residential coal-fired sources) dominates the $PM_{2.5}$-bonded SO_4^{2-} emissions in China. Due to the lack of wet plumes emitted from residential coal combustion, an accurate estimation of sulfate was obtained via indoor simulation (Dai et al., 2019). Thus, re-estimation of the sulfate emissions from industrial coal-fired sources is crucial to evaluate the overall sulfate emissions.

Figure 4 shows the variation in $PM_{2.5}$ and the contained SO_4^{2-} emissions across source sectors in 2017 in mainland China. The actual sulfate emissions, including the plume formation process, are re-evaluated based on the measured data at sites and the deployed proportion of the limestone WFGD technique for CFPPs, industrial boilers, and sintering plants in China. The actual emissions of $PM_{2.5}$ and the contained SO_4^{2-} in 2017 are estimated to be 8.07 ± 0.38 Tg and 0.76 ± 0.09 Tg in total, respectively. The power and industrial sectors contribute ~55.8% to total $PM_{2.5}$ emissions (Zheng et al., 2018); however, these two sectors contribute more than 80% to particulate sulfate emissions when sulfate formation in white plumes is included. An underestimated amount of ~31.4% is attributed to direct SO_4^{2-} formation and the emissions from WFGD applications. In the CFPP sector, contribution underestimations of 67.6% ± 5.5% were found, owing to the widely used limestone-WFGD systems (≥90%) in China (B. Wu et al., 2018). The CFPP sector is the largest contributor to the fine particulate SO_4^{2-} emissions, with a relative proportion of ~35.1%.

The actual production of in-plume sulfate is closely related to the ambient temperature. Estimates of the annual emissions in China based on winter observations may be overestimated due to the relatively low ambient temperature outside stacks and the high operating capacities of the CFPPs in winter. The temporal and spatial distributions of the in-plume sulfate emissions and the SO_2 oxidation mechanism in wet stack plumes, which were difficult to clarify in this study, requires a more detailed study in the future. Due to the difficulty of sampling and measurement in the real world, the number of effective plume samples is

limited. However, the main results obtained through field measurements in this study can provide direct evidence for the further control of flue gas pollution and a better understanding of sulfate formation in the atmosphere.

4. Conclusions

We present the first measurement of freshly formed acidic droplets and sulfate aerosols along the plume edges at the stack outlet in CFPPs, industrial boilers, and sintering plants equipped with WFGD systems. The discharged plume samples after limestone WFGD are extremely acidic (pH = 2.3∼2.8), and SO_4^{2-} accounts for more than half (53%∼77%) of the water-soluble components. Sulfate particles are likely formed during the cooling process of flue gases emitted from WFGD systems and discharged into the ambient air. The majority of the S-rich particles in the plumes are converted from gaseous species, that is, SO_X. The overall calculated sulfate production rates under the NO_2 and TMI-catalyzed oxidation pathways agrees well with the measured data, where the TMI-catalyzed oxidation pathway contributes more than 96% to the calculated sulfate production rate in all wet plumes. When the sulfate formation process in the fresh plumes is considered, the major sulfate precursor (i.e., SO_2) is converted into aerosols during the plume cooling process, especially in CFPPs in winter. Additionally, the in-plume measurement suggests that the CPM results obtained by the dry impinger method (EPA method 202/201A) is commonly underestimated since the fast sulfate process cannot included in the sampling process. The experimental findings improve our basic understanding of the potential environmental impacts of the white plumes and suggest that emitted gaseous pollutants can be converted into sulfate in white plumes ahead of sufficiently diffused in the ambient air. A strategy for the further control of source emitted pollutants by the precooling technique (not a preheating technique) might further reduce the sulfate emissions from industrial plants.

Data Availability Statement

The data sets used in this manuscript were available online (https://figshare.com/articles/dataset/Data_resulting_from_the_study_for_sulfate_explosive_growth_in_wet_plumes_emitted_from_typical_coal-fired_stationary_sources/13688392).

Acknowledgments
We thank Xianmang Xu from Shandong Academy of Sciences, Jianfeng Sun and Chao Zhu from Fudan University, and Ju Wang from Guangdong Hexin Instrument Co., Ltd. We would also like to appreciate Prof. Defeng Zhao from Fudan University, Prof. Huizheng Che from CAMS, Prof. Chuanfeng Zhao from Beijing Normal University, Prof. Jian Gao from Chinese Res Inst Environm Sci, Prof. Guoliang Shi from Nankai University, and Prof. Jingkun Jiang from Tsinghua University. This work was funded by the National Natural Science Foundation of China (21876028 and 91743202).

References

Chen, C., Huang, L., Shi, J., Zhou, Y., Wang, J., Yao, X., et al. (2021). Atmospheric outflow of anthropogenic iron and its deposition to China adjacent seas. *Science of the Total Environment*, *750*, 141302. https://doi.org/10.1016/j.scitotenv.2020.141302

Cheng, Y. F., Zheng, G. J., Wei, C., Mu, Q., Zheng, B., Wang, Z. B., et al. (2016). Reactive nitrogen chemistry in aerosol water as a source of sulfate during haze events in China. *Science Advances*, *2*(12), e1601530-1601540. https://doi.org/10.1126/sciadv.1601530

Connick, R. E., & Zhang, Y.-X. (1996). Kinetics and mechanism of the oxidation of HSO_3^- by O_2. 2. The manganese(II)-catalyzed reaction. *Inorganic Chemistry*, *35*(16), 4613–4621. https://doi.org/10.1021/ic951141i

Dai, Q., Bi, X., Song, W., Li, T., Liu, B., Ding, J., et al. (2019). Residential coal combustion as a source of primary sulfate in Xi'an, China. *Atmospheric Environment*, *196*, 66–76. https://doi.org/10.1016/j.atmosenv.2018.10.002

Dallosto, M., & Harrison, R. (2006). Chemical characterization of single airborne particles in Athens (Greece) by ATOFMS. *Atmospheric Environment*, *40*(39), 7614–7631. https://doi.org/10.1016/j.atmosenv.2006.06.053

Ding, X., Li, Q., Wu, D., Huo, Y., Liang, Y., Wang, H., et al. (2020). Gaseous and garticulate chlorine emissions from typical iron and steel industry in China. *Journal of Geophysical Research: Atmospheres*, *125*(15), e2020JD032729. https://doi.org/10.1029/2020jd032729

Ding, X., Li, Q., Wu, D., Liang, Y., Xu, X., Xie, G., et al. (2019). Unexpectedly increased particle emissions from the steel industry determined by wet/semidry/dry flue gas desulfurization technologies. *Environmental Science and Technology*, *53*(17), 10361–10370. https://doi.org/10.1021/acs.est.9b03081

Dittenhoefer, A. C., & De Pena, R. G. (1980). Sulfate aerosol production and growth in coal-operated power plant plumes. *Journal of Geophysical Research*, *85*(C8), 4499. https://doi.org/10.1029/jc085ic08p04499

Dovrou, E., Rivera-Rios, J. C., Bates, K. H., & Keutsch, F. N. (2019). Sulfate formation via cloud processing from isoprene hydroxyl hydroperoxides (ISOPOOH). *Environmental Science and Technology*, *53*(21), 12476–12484. https://doi.org/10.1021/acs.est.9b04645

Ervens, B. (2015). Modeling the processing of aerosol and trace gases in clouds and fogs. *Chemistry Review*, *115*(10), 4157–4198. https://doi.org/10.1021/cr5005887

Feng, Y., Li, Y., & Cui, L. (2018). Critical review of condensable particulate matter. *Fuel*, *224*, 801–813. https://doi.org/10.1016/j.fuel.2018.03.118

Gen, M., Zhang, R., Huang, D. D., Li, Y., & Chan, C. K. (2019). Heterogeneous SO_2 oxidation in sulfate formation by photolysis of particulate nitrate. *Environmental Science and Technology Letters*, *6*(2), 86–91. https://doi.org/10.1021/acs.estlett.8b00681

Geng, G., Zhang, Q., Tong, D., Li, M., Zheng, Y., Wang, S., & He, K. (2017). Chemical composition of ambient PM2. 5 over China and relationship to precursor emissions during 2005-2012. *Atmospheric Chemistry and Physics*, *17*(14), 9187–9203. https://doi.org/10.5194/acp-17-9187-2017

Green, J. R., Fiddler, M. N., Holloway, J. S., Fibiger, D. L., McDuffie, E. E., Campuzano-Jost, P., et al. (2019). Rates of wintertime atmospheric SO_2 oxidation based on aircraft observations during clear-sky conditions over the Eastern United States. *Journal of Geophysical Research: Atmospheres*, *124*(12), 6630–6649. https://doi.org/10.1029/2018jd030086

Harris, E., Sinha, B., van Pinxteren, D., Tilgner, A., Fomba, K. W., Schneider, J., et al. (2013). Enhanced role of transition metal ion catalysis during in-cloud oxidation of SO_2. *Science*, *340*(6133), 727–730. https://doi.org/10.1126/science.1230911

Huang, R.-J., Zhang, Y., Bozzetti, C., Ho, K.-F., Cao, J.-J., Han, Y., et al. (2014). High secondary aerosol contribution to particulate pollution during haze events in China. *Nature*, *514*(7521), 218–222. https://doi.org/10.1038/nature13774

Karplus, V. J., Zhang, S., & Almond, D. (2018). Quantifying coal power plant responses to tighter SO_2 emissions standards in China. *Proceedings of the National Academy of Sciences of the United States of America*, *115*(27), 7004–7009. https://doi.org/10.1073/pnas.1800605115

Kim, Y. H., Kim, H. S., & Song, C. H. (2017). Development of a reactive plume model for the consideration of power-plant plume photochemistry and its applications. *Environmental Science and Technology*, *51*(3), 1477–1487. https://doi.org/10.1021/acs.est.6b03919

Lei, L., Xie, C., Wang, D., He, Y., Wang, Q., Zhou, W., et al. (2020). Fine particle characterization in a coastal city in China: Composition, sources, and impacts of industrial emissions. *Atmospheric Chemistry and Physics*, *20*(5), 2877–2890. https://doi.org/10.5194/acp-20-2877-2020

Li, J., Wang, X., Chen, J., Zhu, C., Li, W., Li, C., et al. (2017). Chemical composition and droplet size distribution of cloud at the summit of Mount Tai, China. *Atmospheric Chemistry and Physics*, *17*(16), 9885–9896. https://doi.org/10.5194/acp-17-9885-2017

Li, P., Li, X., Yang, C., Wang, X., Chen, J., & Collett, J. L. (2011). Fog water chemistry in Shanghai. *Atmospheric Environment*, *45*(24), 4034–4041. https://doi.org/10.1016/j.atmosenv.2011.04.036

Li, Z., Jiang, J., Ma, Z., Fajardo, O. A., Deng, J., & Duan, L. (2017). Influence of flue gas desulfurization (FGD) installations on emission characteristics of PM 2.5 from coal-fired power plants equipped with selective catalytic reduction (SCR). *Environmental Pollution*, *230*, 655–662. https://doi.org/10.1016/j.envpol.2017.06.103

Liang, Y., Li, Q., Ding, X., Wu, D., Wang, F., Otsuki, T., et al. (2020). Forward ultra-low emission for power plants via wet electrostatic precipitators and newly developed demisters: Filterable and condensable particulate matters. *Atmospheric Environment*, *225*, 117372. https://doi.org/10.1016/j.atmosenv.2020.117372

Lu, Z., Zhang, Q., & Streets, D. G. (2011). Sulfur dioxide and primary carbonaceous aerosol emissions in China and India, 1996-2010. *Atmospheric Chemistry and Physics*, *11*(18), 9839–9864. https://doi.org/10.5194/acp-11-9839-2011

Luria, M., Imhoff, R. E., Valente, R. J., Parkhurst, W. J., & Tanner, R. L. (2001). Rates of conversion of sulfur dioxide to sulfate in a scrubbed power plant plume. *Journal of the Air & Waste Management Association*, *51*(10), 1408–1413. https://doi.org/10.1080/10473289.2001.10464368

Rattigan, O. V., Reilly, J., Judd, C. D., Moore, K. F., Das, M., Sherman, D. E., et al. (2001). Sulfur dioxide oxidation in clouds at Whiteface Mountain as a function of drop size. *Journal of Geophysical Research*, *106*(D15), 17347–17358. https://doi.org/10.1029/2000jd900807

Reff, A., Bhave, P. V., Simon, H., Pace, T. G., Pouliot, G. A., Mobley, J. D., & Houyoux, M. (2009). Emissions inventory of PM2.5 trace elements across the United States. *Environmental Science and Technology*, *43*(15), 5790–5796. https://doi.org/10.1021/es802930x

Seigneur, C., Pai, P., Tombach, I., McDade, C., Saxena, P., & Mueller, P. (2011). Modeling of potential power plant plume impacts on Dallas-Fort Worth visibility. *Journal of the Air & Waste Management Association*, *50*(5), 835–848. https://doi.org/10.1080/10473289.2000.10464121

Shah, V., Jaeglé, L., Thornton, J. A., Lopez-Hilfiker, F. D., Lee, B. H., Schroder, J. C., et al. (2018). Chemical feedbacks weaken the wintertime response of particulate sulfate and nitrate to emissions reductions over the eastern United States. *Proceedings of the National Academy of Sciences of the United States of America*, *115*(32), 8110–8115. https://doi.org/10.1073/pnas.1803295115

Tang, L., Qu, J., Mi, Z., Bo, X., Chang, X., Anadon, L. D., et al. (2019). Substantial emission reductions from Chinese power plants after the introduction of ultra-low emissions standards. *Nature Energy*, *19*, 0468–0477. https://doi.org/10.1038/s41560-019-0468-1

Tong, D., Zhang, Q., Davis, S. J., Liu, F., Zheng, B., Geng, G., et al. (2018). Targeted emission reductions from global super-polluting power plant units. *Nature Sustainability*, *1*(1), 59–68. https://doi.org/10.1038/s41893-017-0003-y

Tsigaridis, K., & Kanakidou, M. (2018). The present and future of secondary organic aerosol direct forcing on climate. *Current Climate Change Report*, *4*(2), 84–98. https://doi.org/10.1007/s40641-018-0092-3

Wang, G., Deng, J., Zhang, Y., Li, Y., Ma, Z., Hao, J., & Jiang, J. (2020). Evaluating airborne condensable particulate matter measurement methods in typical stationary sources in China. *Environmental Science and Technology*, *54*(3), 1363–1371. https://doi.org/10.1021/acs.est.9b05282

Wang, J., Li, J., Ye, J., Zhao, J., Wu, Y., Hu, J., et al. (2020). Fast sulfate formation from oxidation of SO_2 by NO_2 and HONO observed in Beijing haze. *Nature Communications*, *11*(1), 2844. https://doi.org/10.1038/s41467-020-16683-x

Wang, X., Chen, J., Sun, J., Li, W., Yang, L., Wen, L., et al. (2014). Severe haze episodes and seriously polluted fog water in Ji'nan, China. *Science of the Total Environment*, *493*, 133–137. https://doi.org/10.1016/j.scitotenv.2014.05.135

Wang, Y. X., Zhang, Q. Q., Jiang, J. K., Zhou, W., Wang, B. Y., He, K. B., et al. (2014). Enhanced sulfate formation during China's severe winter haze episode in January 2013 missing from current models. *Journal of Geophysical Research: Atmospheres*, *119*(17), 10425–10440. https://doi.org/10.1002/2013jd021426

Wu, B., Bai, X., Liu, W., Lin, S., Liu, S., Luo, L., et al. (2020). Non-negligible stack emissions of noncriteria air pollutants from coal-fired power plants in China: Condensable particulate matter and sulfur trioxide. *Environmental Science and Technology*, *54*(11), 6540–6550. https://doi.org/10.1021/acs.est.0c00297

Wu, B., Tian, H., Hao, Y., Liu, S., Liu, X., Liu, W., et al. (2018). Effects of wet flue gas desulfurization and wet electrostatic precipitators on emission characteristics of particulate matter and its ionic compositions from four 300 MW level ultralow coal-fired power plants. *Environmental Science and Technology*, *52*(23), 14015–14026. https://doi.org/10.1021/acs.est.8b03656

Wu, D., Li, Q., Ding, X., Sun, J., Li, D., Fu, H., et al. (2018). Primary particulate matter emitted from heavy fuel and diesel oil combustion in a typical container ship: Characteristics and toxicity. *Environmental Science and Technology*, *52*(21), 12943–12951. https://doi.org/10.1021/acs.est.8b04471

Xue, J., Yuan, Z., Griffith, S. M., Yu, X., Lau, A. K. H., & Yu, J. Z. (2016). Sulfate formation enhanced by a cocktail of high NOx, SO_2, particulate matter, and droplet pH during haze-fog events in megacities in China: An observation-based modeling investigation. *Environmental Science and Technology*, *50*(14), 7325–7334. https://doi.org/10.1021/acs.est.6b00768

Yang, J., Ma, S., Gao, B., Li, X., Zhang, Y., Cai, J., et al. (2017). Single particle mass spectral signatures from vehicle exhaust particles and the source apportionment of on-line PM 2.5 by single particle aerosol mass spectrometry. *Science of the Total Environment*, *593–594*, 310–318. https://doi.org/10.1016/j.scitotenv.2017.03.099

Zhang, R., Wang, G., Guo, S., Zamora, M. L., Ying, Q., Lin, Y., et al. (2015). Formation of urban fine particulate matter. *Chemistry Review*, *115*(10), 3803–3855. https://doi.org/10.1021/acs.chemrev.5b00067

Zhang, Y., Cai, J., Wang, S., He, K., & Zheng, M. (2017). Review of receptor-based source apportionment research of fine particulate matter and its challenges in China. *Science of the Total Environment*, *586*, 917–929. https://doi.org/10.1016/j.scitotenv.2017.02.071

Zhang, Y., Yao, Z., Shen, X., Liu, H., & He, K. (2015). Chemical characterization of PM 2.5 emitted from on-road heavy-duty diesel trucks in China. *Atmospheric Environment*, *122*, 885–891. https://doi.org/10.1016/j.atmosenv.2015.07.014

Zheng, B., Tong, D., Li, M., Liu, F., Hong, C., Geng, G., et al. (2018). Trends in China's anthropogenic emissions since 2010 as the consequence of clean air actions. *Atmospheric Chemistry and Physics*, *18*(19), 14095–14111. https://doi.org/10.5194/acp-18-14095-2018

Zheng, G., Su, H., Wang, S., Andreae, M. O., Pöschl, U., & Cheng, Y. (2020). Multiphase buffer theory explains contrasts in atmospheric aerosol acidity. *Science*, *369*(6509), 1374–1377. https://doi.org/10.1126/science.aba3719

Zhou, Y., Zhang, Y., Griffith, S. M., Wu, G., Li, L., Zhao, Y., et al. (2020). Field evidence of Fe-mediated photochemical degradation of oxalate and subsequent sulfate formation observed by single particle mass spectrometry. *Environmental Science and Technology*, *54*(11), 6562–6574. https://doi.org/10.1021/acs.est.0c00443

References From the Supporting Information

Chen, P., Wang, T., Dong, M., Kasoar, M., Han, Y., Xie, M., et al. (2017). Characterization of major natural and anthropogenic source profiles for size-fractionated PM in Yangtze River Delta. *Science of the Total Environment*, *598*, 135–145. https://doi.org/10.1016/j.scitotenv.2017.04.106

Chen, X., Liu, Q., Yuan, C., Sheng, T., Zhang, X., Han, D., et al. (2019). Emission characteristics of fine particulate matter from ultra-low emission power plants. *Environmental Pollution*, *255*, 113157. https://doi.org/10.1016/j.envpol.2019.113157

Cui, M., Chen, Y., Feng, Y., Li, C., Zheng, J., Tian, C., et al. (2017). Measurement of PM and its chemical composition in real-world emissions from non-road and on-road diesel vehicles. *Atmospheric Chemistry and Physics*, *17*(11), 6779–6795. https://doi.org/10.5194/acp-17-6779-2017

Fujita, E. M., Campbell, D. E., Arnott, W. P., Chow, J. C., & Zielinska, B. (2007). Evaluations of the chemical mass balance method for determining contributions of gasoline and diesel exhaust to ambient carbonaceous aerosols. *Journal of the Air & Waste Management Association*, *57*(6), 721–740. https://doi.org/10.3155/1047-3289.57.6.721

Guo, Y., Gao, X., Zhu, T., Luo, L., & Zheng, Y. (2017). Chemical profiles of PM emitted from the iron and steel industry in northern China. *Atmospheric Environment*, *150*, 187–197. https://doi.org/10.1016/j.atmosenv.2016.11.055

Hao, Y., Gao, C., Deng, S., Yuan, M., Song, W., Lu, Z., & Qiu, Z. (2019). Chemical characterization of PM2.5 emitted from motor vehicles powered by diesel, gasoline, natural gas and methanol fuel. *Science of the Total Environment*, *674*, 128–139. https://doi.org/10.1016/j.scitotenv.2019.03.410

Hong, L., Liu, G., Zhou, L., Li, J., Xu, H., & Wu, D. (2017). Emission of organic carbon, elemental carbon and water-soluble ions from crop straw burning under flaming and smoldering conditions. *Particuology*, *31*, 181–190. https://doi.org/10.1016/j.partic.2016.09.002

Ibusuki, T., & Takeuchi, K. (1987). Sulfur dioxide oxidation by oxygen catalyzed by mixtures of manganese(II) and iron(III) in aqueous solutions at environmental reaction conditions. *Atmospheric Environment*, *21*(7), 1555–1560. https://doi.org/10.1016/0004-6981(87)90317-9

Jaiprakash, & Habib, G. (2017). Chemical and optical properties of PM2.5 from on-road operation of light duty vehicles in Delhi city. *Science of the Total Environment*, *586*, 900–916. https://doi.org/10.1016/j.scitotenv.2017.02.070

Jia, J., Cheng, S., Yao, S., Xu, T., Zhang, T., Ma, Y., et al. (2018). Emission characteristics and chemical components of size-segregated particulate matter in iron and steel industry. *Atmospheric Environment*, *182*, 115–127. https://doi.org/10.1016/j.atmosenv.2018.03.051

Kim Oanh, N. T., Thiansathit, W., Bond, T. C., Subramanian, R., Winijkul, E., & Paw-armart, I. (2010). Compositional characterization of PM2.5 emitted from in-use diesel vehicles. *Atmospheric Environment*, *44*(1), 15–22. https://doi.org/10.1016/j.atmosenv.2009.10.005

Lee, Y., & Schwartz, S. E. (1983). Kinetics of oxidation of aqueous sulfur(IV) by nitrogen dioxide. In H. R. Pruppacher, R. G. Semonin, & W. G. N. Slinn (Eds.), Precipitation scavenging, dry deposition and resuspension (1). Elsevier. Retrieved from https://www.osti.gov/biblio/6567096

Li, J., Zhu, C., Chen, H., Fu, H., Xiao, H., Wang, X., et al. (2020). A more important role for the Ozone-S(IV) oxidation pathway due to decreasing acidity in clouds. *Journal of Geophysical Research: Atmospheres*, *125*(18), e2020JD033220. https://doi.org/10.1029/2020jd033220

Li, X., Wang, S., Duan, L., Hao, J., & Nie, Y. (2009). Carbonaceous aerosol emissions from household biofuel combustion in China. *Environmental Science and Technology*, *43*(15), 6076–6081. https://doi.org/10.1021/es803330j

Liu, H. B., Kong, S. F., Wang, W., & Yan, Q. (2016). Emission inventory of heavy metals in fine particles emitted from residential coal burning in China. *Environmental Sciences*, *37*(8), 13. https://doi.org/10.13277/j.hjkx.2016.08.002

Liu, Y., Zhang, W., Bai, Z., Yang, W., Zhao, X., Han, B., & Wang, X. (2017). Characteristics of $PM_{2.5}$ chemical source profiles of coal combustion and industrial process in China. *Research of Environmental Sciences*, *12*, 1859–1868. https://doi.org/10.13198/j.issn.1001-6929.2017.03.34

Liu, Y., Zhang, W., Yang, W., Bai, Z., & Zhao, X. (2018). Chemical compositions of $PM_{2.5}$ emitted from diesel trucks and construction equipment. *Aerosol Science and Engineering*, *2*(2), 10. https://doi.org/10.1007/s41810-017-0020-2

Ma, Z., Li, Z., Jiang, J., Deng, J., Zhao, Y., Wang, S., & Duan, L. (2017). PM2.5 emission reduction by technical improvement in a typical coal-fired power plant in China. *Aerosol and Air Quality Research*, *17*(2), 636–643. https://doi.org/10.4209/aaqr.2016.05.0200

Pei, B., Wang, X., Zhang, Y., Hu, M., Sun, Y., Deng, J., et al. (2016). Emissions and source profiles of PM2.5 for coal-fired boilers in the Shanghai megacity, China. *Atmospheric Pollution Research*, *7*(4), 577–584. https://doi.org/10.1016/j.apr.2016.01.005

Ruan, R., Liu, H., Tan, H., Yang, F., Li, Y., Duan, Y., et al. (2019). Effects of APCDs on PM emission: A case study of a 660 MW coal-fired unit with ultralow pollutants emission. *Applied Thermal Engineering*, *155*, 418–427. https://doi.org/10.1016/j.applthermaleng.2019.03.136

Ruan, R., Xu, X., Tan, H., Zhang, S., Lu, X., Zhang, P., et al. (2019). Emission characteristics of particulate matter from two ultralow-emission coal-fired industrial boilers in Xi'an, China. *Energy & Fuels*, *33*(3), 1944–1954. https://doi.org/10.1021/acs.energyfuels.8b04069

Spindler, G., Hesper, J., Brüggemann, E., Dubois, R., Müller, T., & Herrmann, H. (2003). Wet annular denuder measurements of nitrous acid: Laboratory study of the artifact reaction of NO_2 with S(IV) in aqueous solution and comparison with field measurements. *Atmospheric Environment*, *37*(19), 2643–2662. https://doi.org/10.1016/s1352-2310(03)00209-7

Xia, Y. J., Huang, X. M., Song, W. B., Yang, N. W., & Yang, Y. L. (2017). Components of $PM_{2.5}$ and PM_{10} in coal fired boiler particulate matter of Xi'an City. *Huan jing wu ran yu fang zhi*, *039*(002), 207–211. https://doi.org/10.15985/j.cnki.1001-3865.2017.02

Zheng, M., Zhang, Y., Yan, C., Fu, H., Niu, H., Huang, K., et al. (2013). Establishing $PM_{2.5}$ industrial source profiles in Shanghai. *China Environmental Science*, *33*(8), 1354–1359.